Available online at www.sciencedirect.com
SCIENCE DIRECT
Schizophrenia Research 76 (2005) 337–342
SCHIZOPHRENIA RESEARCH
www.elsevier.com/locate/schres

Advanced paternal age associated with an elevated risk for schizophrenia in offspring in a Japanese population

Kenji J. Tsuchiya[a], Shu Takagai[a], Masayoshi Kawai[a], Hideo Matsumoto[b], Kazuhiko Nakamura[a], Yoshio Minabe[a], Norio Mori[a], Nori Takei[a,c,*]

[a]*Department of Psychiatry and Neurology, Hamamatsu University School of Medicine, Hamamatsu, Japan*
[b]*Department of Psychiatry, Tokai University School of Medicine, Isehara, Japan*
[c]*Division of Psychological Medicine, Institute of Psychiatry, London, UK*

Received 14 December 2004; received in revised form 2 March 2005; accepted 4 March 2005
Available online 21 April 2005

Abstract

Objective: Advanced paternal age at birth as a risk for schizophrenia in the adult offspring has been reported in previous studies exclusively conducted in Western countries and Israel. The question has arisen whether this finding could be replicated in countries with socially and culturally different attitudes toward marriage, including factors such as age at marriage. To address this question, we conducted a case-control study of a Japanese population.
Methods: The subjects were representative inpatients with a DSM-IV diagnosis of schizophrenia. Unrelated healthy volunteers were recruited as control subjects. This study was conducted as one of a series of the projects by use of "The Mother and Child Health Handbooks (MCHHs)," from which information on parental characteristics around the time of birth, including parental ages at birth, had been extracted and recorded on computer.
Results: Ninety-nine subjects with schizophrenia and 381 healthy control subjects enrolled for the study. Advanced paternal, but not maternal, age was associated with an elevated risk for schizophrenia. Reproducibility of the association across different cultures is suggestive of a causal link.

Keywords: Schizophrenia; Paternal age; Risk factor; Case-control study; Japan

1. Introduction

Recent studies have consistently reported that advanced paternal age at birth is a risk factor for schizophrenia in the offspring (Brown et al., 2002; Byrne et al., 2003; Dalman and Allebeck, 2002; El Saadi et al., 2004; Malaspina et al., 2001; Zammit et al., 2003). Paternal germ line mutation may be a likely

* Corresponding author. Department of Psychiatry and Neurology, Hamamatsu University School of Medicine, 1-20-1 Handayama, Hamamatsu 431-3192, Japan. Tel.: +81 53 435 2295; fax: +81 53 435 3621.
E-mail address: ntakei@hama-med.ac.jp (N. Takei).

0920-9964/$ - see front matter © 2005 Elsevier B.V. All rights reserved.
doi:10.1016/j.schres.2005.03.004

explanation (Malaspina, 2001), but the mechanism underlying this association is not yet fully understood.

Previous studies examining this association have been conducted exclusively in European countries, Israel, USA, and Australia. Attitudes toward marriage, in particular, age at the time of marriage, may vary according to cultural backgrounds. If the association between advanced paternal age and the risk for schizophrenia were reproduced among populations of different ethnic origin, the relationship addressed here would be more indicative of causal significance, and genetic explanations including de novo mutation on schizophrenia-susceptible genes would become realistic (Malaspina, 2001).

Therefore, we investigated whether or not the claimed association between advanced paternal age at birth and the risk for schizophrenia among offspring would be reproducible in a Japanese population.

2. Methods

This study was conducted as a series of our projects which were launched to investigate pregnancy- and birth-related events as risk factors for schizophrenia in Japan. The projects were set out to exclusively utilize the Mother and Child Health Handbook (MCHH), a set of notes covering a wide range of information, including pregnancy and delivery events, as well as newborns' characteristics and parental data. In Japan, every woman receives the MCHH from the local municipal office when pregnant and, in general, keeps it long after the birth of the offspring as a memorial. Ample information derived from the MCHHs has been systematically recorded on computer and, thus far, used for a series of studies (Kawai et al., 2004; Matsumoto et al., 1999, 2001).

We sought the participation of subjects with schizophrenia who were admitted to the University Hospital of the Hamamatsu University School of Medicine during the period extending from January 1, 1999 to December 31, 2002. A structured interview was conducted by trained psychiatrists (K.J.T., K.M., N.M. and N.T.) using the Schedule for Clinical Interview for Axis-I Diagnosis of DSM-IV (SCID-I) (First et al., 1996). Those individuals, who met the criteria for a DSM-IV diagnosis of schizophrenia (295.xx) and whose biological mothers were identified, were recruited. We also included unrelated healthy volunteers who were residents in the community from which the patient group was derived, and who were confirmed to have had no psychiatric history.

As regards the parental age and parity, we relied upon computerized MCHH data. As these data have become available since the year 1967, only individuals born in and after 1968 were included in the present study. Maternal and paternal ages were divided into tertiles according to the distribution of age (see Table 1). The family history of psychiatric diagnoses was examined via interviews with each subject and one close relative, most often the mother; subjects were designated as "positive" for a psychiatric family history if they had at least one first-degree relative with psychosis. Odds ratios (ORs) and

Table 1
Odds ratios for schizophrenia among offspring in relation to parental age

	Cases ($n=99$)	Controls ($n=381$)	Crude estimates		Adjusted estimates[a]	
			ORs	95% CI	ORs	95% CI
Maternal age (year)						
≦25 (reference)	31	128	1		1	
26–28	40	118	1.40	(0.82, 2.38)	1.08	(0.60, 1.93)
≧29	28	135	0.86	(0.49, 1.51)	0.59	(0.29, 1.20)
Test for trend			$p=0.60$		$p=0.14$	
Paternal age (year)						
≦28 (reference)	22	138	1		1	
29–31	36	120	1.88	(1.05, 3.37)	2.08	(1.12, 3.86)
≧32	41	123	2.09	(1.18, 3.71)	3.00	(1.49, 6.04)
Test for trend			$p=0.013$		$p=0.002$	

[a] Adjusted for age and gender of the subject, parity, family history, and age of the other parent.

95% confidence intervals (CIs) for schizophrenia in relation to parental age categories were estimated using logistic regression. Along with the crude OR, we computed the OR adjusted for relevant covariates in order to eliminate the confounding effects. In light of the moderate sample size of the present study, we opted for a parsimonious model to increase precision rather than a model in which all available variables were adjusted for. We adopted a logistic regression model with a forward procedure (Kleinbaum et al., 1998). Following the recommendation by Kleinbaum et al. (1998), we chose a loosened alpha level of .20 to include potential confounders in the model. For the statistical analyses, we used STATA, version 8.1 (Stata Corporation, 2003).

Written informed consent was obtained from each participant. This study design was approved by the University Hospital Ethics Committee.

3. Results

3.1. Characteristics in patients and controls

Ninety-nine patients with schizophrenia and 381 control subjects participated in this study. The mean age differed significantly between the patients and controls (25.4 years [S.D. 5.5] for the patients and 23.0 years [S.D. 4.3] for the controls; $t=4.53$, $df=478$, $p<.001$). More male subjects were included among the patients ($n=56$, 57%) than among the controls ($n=179$, 47%); $\chi^2=2.89$, $df=1$, $p=.089$. A higher proportion of a family history of psychosis was noted among the patients (8/99, 8%) than among the controls (14/381, 4%); $\chi^2=3.49$, $df=1$, $p=.062$. There was no marked or significant difference in the distribution of first-born subjects between the patients (40/99, 40%) and controls (157/381, 41%); $\chi^2=0.02$, $df=1$, $p=.89$.

3.2. Parental age and risk for schizophrenia in the offspring

Maternal age at birth did not differ significantly between the two groups (27.3 years [S.D. 3.5] for the patients and 27.3 years [S.D. 3.5] for the controls; $t=0.12$, $df=478$, $p=.91$); however, there was a trend toward greater paternal age at birth among the patients with schizophrenia than among the controls (30.9 years [S.D. 3.7] for the patients and 30.1 years [S.D. 4.0] for the controls; $t=1.87$, $df=478$, $p=.062$).

Differences in risk were then examined across three classes of maternal age at birth using logistic regression with no adjustment for covariates; the test for a linear trend revealed no association (likelihood ratio test (LRT)=0.28, $df=1$, $p=.60$) (Table 1). However, as regards paternal age, the test for a linear trend did reveal a significant association (LRT=6.28, $df=1$, $p=.013$). Those subjects whose paternal age was 29 to 31 years at birth had a 1.9-fold increased risk, and those with a paternal age of 32 years or older had a 2.1-fold increased risk, compared to those with a paternal age of 28 years or younger.

Subsequently, we incorporated potential confounding factors into the logistic regression model with a forward procedure, as described above. Accordingly, age, sex, family history, and age of the other parent were entered into the model as covariates. The linear trend that had been observed in the crude analysis of paternal age remained significant, but became even more significant after adjustment for these covariates (LRT=9.37, $df=1$, $p=.002$). In effect, the estimated risk among the offspring of the highest paternal age class was three times greater than that of the offspring of the lowest paternal age class. However, as for maternal age, no association emerged, even after the covariates were entered into the model (LRT=2.21, $df=1$, $p=.14$).

A third factor in the context of the relationship between two factors (paternal age and a risk for the disorder) may account for the implication of advanced paternal age as a risk factor, i.e., deviation in paternal behavior. Namely, men with a predisposition to the disorder may tend to get married and to father children at a relatively high age. As information on the behavioral traits of the fathers of the subjects included in the present study was not available, we chose to examine the interaction of "family history" and "paternal age" in the same regression model. In this analysis, we found no significant interaction effect (LRT=1.40, $df=1$, $p=.24$).

4. Discussion

In the Japanese population, we found an association between advanced paternal age at birth and the

risk for schizophrenia in the offspring. This finding is consistent with that of previous studies (Brown et al., 2002; Byrne et al., 2003; Dalman and Allebeck, 2002; El Saadi et al., 2004; Malaspina et al., 2001; Zammit et al., 2003). However, these prior studies did not find support for an association between maternal age and the risk of offspring developing the disorder. The results of the present study also showed no such association, and are hence once again in agreement with previous reports.

It is highly likely that marital habits, including preferred age at marriage among men, as well as fathering age, vary across countries and cultures. In fact, the mean paternal age at birth in a Swedish study was 32.2 years for control offspring (Zammit et al., 2003), which was slightly older than that (31.5 years) in an Israeli study (Malaspina et al., 2001) (information on mean paternal age is not available in the other studies cited above). In contrast, our Japanese study showed a comparatively younger paternal age at birth (30.1 years) in the control subjects. These data indicate some degree of cultural influence on fathering age. Nevertheless, all of the previous studies cited here, as well as our study, showed the same finding of an association between paternal age at birth and the risk for schizophrenia, strongly suggesting the presence of non-culturally determined factor(s).

Apart from cultural factors, other technical issues, in particular the diagnosis, need to be considered. Previous studies have employed several different definitions of schizophrenia, including broadly defined psychoses as well as schizophrenia within a "narrow" framework; each of the definitions employed may exert a different impact on the association of interest. As regards studies utilizing a broad concept of psychosis that includes schizophrenia, four studies incorporated subsamples with psychoses, namely affective psychosis as well as non-affective psychosis (three parts of the study by El Saadi et al., 2004; Brown et al., 2002). Among these studies, two studies showed a significant association between advanced paternal age and risk (the Swedish and Danish part of the study by El Saadi et al., 2004), and one study showed a trend toward the association (Brown et al., 2002), although the remaining study did not find support for the association (the Australian part of the study by El Saadi et al., 2004). Therefore, the reported findings remain inconsistent. On the other hand, four studies investigated subjects with "narrow" schizophrenia (e.g., 295 in ICD-9 or F20 in ICD-10), and all showed a significant association (Brown et al., 2002; Dalman and Allebeck, 2002; Zammit et al., 2003; Byrne et al., 2003).

In this context, of particular interest is a study by Brown et al. (2002), who directly compared the strength of the association according to the diagnoses opted for (i.e., psychoses vs. schizophrenia). They demonstrated that the relative risk for schizophrenia among individuals with oldest fathers at birth (45 years or over) was 3.6 (95% CI: 1.0 to 15.5), whereas the relative risk for psychoses among those with fathers belonging to the same age class was 2.7 (95% CI: 0.8 to 7.2), compared with those with the youngest fathers of 15–24 years. These findings indicate that the use of narrowly defined schizophrenia strengthens the association. Strictly speaking, as we adopted a DSM-IV diagnosis of schizophrenia, our findings can only be compared with those studies which adopted a similar (i.e., "narrow") definition (Brown et al., 2002; Byrne et al., 2003; Dalman and Allebeck, 2002; Zammit et al., 2003). All such studies, including ours, provide supportive evidence for the conclusion that advanced paternal age is associated with an increased risk for schizophrenia among the offspring. In addition, two studies have shown that the paternal age effect is stronger for schizophrenia than for psychoses other than schizophrenia (Malaspina et al., 2001; Zammit et al., 2003). Therefore, it is likely that advanced paternal age is more specifically related to schizophrenia than to other types of psychosis.

Another important factor that may have influenced our findings is birth order. Naturally, later-born children are likely to have an older father compared to first-born children. A study has reported that later birth order is associated with an increased risk for schizophrenia (Sham et al., 1993). Thus, some of the present findings might have been partly due to the effect of birth order. Among all the subjects in the present study, the mean paternal age at the birth of the first-born children was significantly younger, i.e., 28.5 years (S.D. 3.1), compared to that of the fathers of the later-born children, i.e., 31.5 years (S.D. 4.0) ($t=8.80$, $df=478$, $p<.001$). However, parity (or birth order) was not associated with an increased risk for the disorder (first-born vs. later-born, LRT=0.02, $df=1$, $p=0.89$; OR=0.97 [95% CI: 0.62 to 1.52]). Furthermore, in order to rule out any residual

confounding effect of birth order, we adjusted for this factor in our logistic regression model.

On the other hand, the behavioral characteristics of the fathers might account for the association we found between advanced paternal age and a risk for schizophrenia in the offspring. Many studies have indicated that "schizotypy", or schizotypal personality traits reflect a genetic background of schizophrenia and run in the pedigree of patients with the disorder (Kendler et al., 1995; Mata et al., 2000). The behavior of fathers with such traits may be characterized by impaired sociality, which may lead to relatively late marriage. Therefore, our finding of advanced paternal age at birth in the pre-schizophrenic offspring could be accounted for by their father's behavioral characteristics. However, such a scenario of genetic influence should equally pertain to the maternal side, that is, maternal behavioral characteristics. We found no association of maternal age with the risk, which is opposed to the genetic account of the finding in this study. In addition, the ORs representing the strength of the association between paternal age and the risk remained unchanged after adjustment for a family history of psychosis. Moreover, no interaction effect of family history and the paternal age was evident. In accord with these findings, a study by Byrne et al. (2003), who examined two risk sets (all subjects and subjects without a family history of psychiatric diagnosis), has shown that the strength of the association between advanced paternal age and the risk for schizophrenia does not differ between the two sets of the sample. Therefore, it is unlikely that the association between advanced paternal age and the risk for schizophrenia is explained exclusively by family history, or by paternal "schizotypy".

A different approach has also been applied to address the relation of family history to the paternal age effect. Malaspina et al. (2002) examined the paternal age separately for schizophrenia probands with at least one first- or second-degree relative suffering from non-affective psychosis (i.e., familial schizophrenia) and those without such relatives (i.e., sporadic schizophrenia). This was conducted on the basis that if paternal age were older in sporadic cases than in familial cases, then new germ line mutations would be a possible explanation for the paternal age effect. Indeed, the results provided evidence supporting their prediction (Malaspina et al., 2002). However, this finding was not supported by a recent study of Pulver et al. (2004), who also investigated parental age at birth in familial vs. sporadic cases, and found no group difference. Although the findings of the two studies conflict with each other, they, at the very least, do not give support to a genetic link between the paternal age at birth and the risk of the disorder.

It should be noted that Dalman and Allebeck (2002) reported that those individuals with fathers belonging to the oldest age class or to the youngest age class at birth may be associated with an increased risk, compared to those with fathers belonging to the middle age class. We failed to replicate such a 'U'-shaped relationship of paternal age to the risk for the disorder; instead, our findings indicated a linear relationship between advanced paternal age and the risk for schizophrenia.

4.1. Limitations and strengths

We only used three age classes for categorizing paternal age. In order to scrutinize the possible U-shaped relationship discussed above, more age classes would be optimal. This was, however, hampered due to the relatively small sample sizes in our study. In this regard, large studies are clearly of benefit. As regards the evaluation of family history, we did not conduct a structured interview for the evaluation of each of the subject's relatives. We therefore might have misclassified the status of family history, and this misclassification may have in turn obscured the true genetic influence on the risk association explored here.

On the other hand, the ethnic composition of the present sample was homogenous; that is, all of the subjects recruited for this study were Japanese and had been born in Japan. This is the first replication study on this topic conducted in an Asian country, and such reproducibility implies that the risk-increasing effect of advanced paternal age at birth is observable across different cultures, which further enhances the likelihood of a true association.

Acknowledgments

A part of this study was presented at the 12th Biennial Winter Workshop for Schizophrenia, Davos,

Switzerland, on February 10, 2004. This study was financially supported by a Grant-in-Aid for Scientific Research from the Ministry of Education, Culture, Sports, Science and Technology, Japan: Dr. Takei is a recipient of a Grant-in-Aid for Science Research (B) (2) No. 14370288. The authors would also like to thank Christina Dalman, MD, PhD, for her helpful comments.

References

Brown, A.S., Schaefer, C.A., Wyatt, R.J., Begg, M.D., Goetz, R., Bresnahan, M.A., Harkavy-Friedman, J., Gorman, J.M., Malaspina, D., Susser, E.S., 2002. Paternal age and risk of schizophrenia in adult offspring. Am. J. Psychiatry 159, 1528–1533.

Byrne, M., Agerbo, E., Ewald, H., Eaton, W.W., Mortensen, P.B., 2003. Parental age and risk of schizophrenia: a case-control study. Arch. Gen. Psychiatry 60, 673–678.

Dalman, C., Allebeck, P., 2002. Paternal age and schizophrenia: further support for an association. Am. J. Psychiatry 159, 1591–1592.

El Saadi, O., Pedersen, C.B., McNeil, T.F., Saha, S., Welham, J., O'Callaghan, E., Cantor-Graae, E., Chant, D., Mortensen, P.B., McGrath, J., 2004. Paternal and maternal age as risk factors for psychosis: findings from Denmark, Sweden and Australia. Schizophr. Res. 67, 227–236.

First, M.B., Spitzer, R.L., Gibbon, M., Williams, J.B.W., 1996. Structured Clinical Interview for DSM-IV Axis I Disorders (Version 2.0). American Psychiatric Publishing Inc., Arlington, VA. (Japanese translation by S. Takahashi, Japan UNI Agency Inc. Tokyo).

Kawai, M., Minabe, Y., Takagai, S., Ogai, M., Matsumoto, H., Mori, N., Takei, N., 2004. Poor maternal care and high maternal body mass index in pregnancy as a risk factor for schizophrenia in offspring. Acta Psychiatr. Scand. 110, 257–263.

Kendler, K.S., McGuire, M., Gruenberg, A.M., Walsh, D., 1995. Schizotypal symptoms and signs in the Roscommon family study. Their factor structure and familial relationship with psychotic and affective disorders. Arch. Gen. Psychiatry 52, 296–303.

Kleinbaum, D.G., Kupper, L.L., Muller, K.E., Nizam, A., 1998. Applied Regression Analysis and Other Multivariable Methods, 3rd ed. Duxberry Press, Pacific Grove, CA.

Malaspina, D., 2001. Paternal factors and schizophrenia risk: de novo mutations and imprinting. Schizophr. Bull. 27, 379–393.

Malaspina, D., Harlap, S., Fennig, S., Heiman, D., Nahon, D., Feldman, D., Susser, E.S., 2001. Advancing paternal age and the risk of schizophrenia. Arch. Gen. Psychiatry 58, 361–367.

Malaspina, D., Corcoran, C., Fahim, C., Berman, A., Harkavy-Friedman, J., Yale, S., Goetz, D., Goetz, R., Harlap, S., Gorman, J., 2002. Paternal age and sporadic schizophrenia: evidence for de novo mutations. Am. J. Med. Genet. 114, 299–303.

Mata, I., Sham, P.C., Gilvarry, C.M., Jones, P.B., Lewis, S.W., Murray, R.M., 2000. Childhood schizotypy and positive symptoms in schizophrenic patients predict schizotypy in relatives. Schizophr. Res. 44, 129–136.

Matsumoto, H., Takei, N., Saito, H., Kachi, K., Mori, N., 1999. Childhood-onset schizophrenia and obstetric complications: a case-control study. Schizophr. Res. 38, 93–99.

Matsumoto, H., Takei, N., Saito, H., Kachi, K., Mori, N., 2001. The association between obstetric complications and childhood-onset schizophrenia: a replication study. Psychol. Med. 31, 907–914.

Pulver, A.E., McGrath, J.A., Liang, K.Y., Lasseter, V.K., Nestadt, G., Wolyniec, P.S., 2004. An indirect test of the new mutation hypothesis associating advanced paternal age with the etiology of schizophrenia. Am. J. Med. Genet. 124B, 6–9.

Sham, P.C., MacLean, C.J., Kendler, K.S., 1993. Risk of schizophrenia and age difference with older siblings. Evidence for a maternal viral infection hypothesis? Br. J. Psychiatry 163, 627–633.

Stata Corporation,, 2003. Stata Special Edition Version 8.1 for Windows. Strata Corporation, College Station, TX.

Zammit, S., Allebeck, P., Dalman, C., Lundberg, I., Hemmingson, T., Owen, M.J., Lewis, G., 2003. Paternal age and risk for schizophrenia. Br. J. Psychiatry 183, 405–408.

Available online at www.sciencedirect.com
SCIENCE DIRECT®
Cognitive Brain Research 23 (2005) 164–170
COGNITIVE BRAIN RESEARCH
www.elsevier.com/locate/cogbrainres

Research report

Neural substrates in judgment process while playing go: a comparison of amateurs with professionals

Yasuomi Ouchi[a,*], Toshihiko Kanno[a], Etsuji Yoshikawa[b], Masami Futatsubashi[b], Hiroyuki Okada[b], Tatsuo Torizuka[a], Mitsuo Kaneko[a]

[a]*Positron Medical Center, Hamamatsu Medical Center, 5000 Hirakuchi, Hamakita, 434-0041, Japan*
[b]*Central Research Laboratory, Hamamatsu Photonics K.K. Hamakita, 434-8601, Japan*

Accepted 15 October 2004
Available online 10 November 2004

Abstract

A professional go player shows incomparable ability in judgment during go game. Positron emission tomography (PET) was used to investigate the neural substrates of professional go player's judgment process. Eight professional go players and six amateur players were instructed to think over silently in the opening-stage game (*fuseki*, territorial planning) problems and the life-or-death (*tsume*, checkmate judgment) problems presented on the monitor in front of them for 60 s of $H_2^{15}O$ PET scans and to state the answer afterwards. We found that in the territorial planning problems the parietal activation was equally observed in both groups with the additional prefrontal activation in the amateur group, and in the checkmate-decision problems the precuneus and cerebellum were activated in professionals while the premotor and parietooccipital cortices (visuospatial processing region) were extensively activated in amateurs. The comparison of the two groups showed stronger activations in the precuneus and cerebellum in the professionals in contrast to the premotor activation in amateurs during checkmate judgment. In addition, the cerebellum was remarkably activated in the higher ranking professional players. These findings suggested the cerebellum and precuneus play important roles in processing of accurate judgment by visual imagery and nonmotor learning memory processes in professional go players.

Theme: Neural basis of behavior
Topic: Cognition

Keywords: Go; Professional; Judgment; Precuneus; Cerebellum; Positron emission tomography

1. Introduction

There are several neuroimaging studies concerning the neural substrates of cognitive processes involved in professional thinking [13,20,25]. In these studies, the contribution of the prefrontal and parietal cortices was reported to be of great importance. Specifically, the precuneus was remarkably activated during the execution of precise topographical memory recall for professional taxi drivers [20] and in visuospatial processing for abacus experts [13]. In addition to these cerebral activations in cognitive processes, recent findings on the cerebellum in nonmotor cognitive processes are worth noticing because the cerebellum is activated in many other cognitive tasks such as memory, error detection, attention, sensory discrimination and timing [1,2,10,15,18]. Furthermore, since the cerebellum also functions under the condition of the theory of mind [5], it is easy to speculate that an expert would exploit this "cognitive organ" more efficiently in cognitive tasks. However, this issue remains to be investigated.

The game go involves similar thought processes as the Western-style board game of chess. A previous activation study during a chess game revealed neural substrates of

* Corresponding author. Fax: +81 53 585 0367.
E-mail address: ouchi@pmc.hmedc.or.jp (Y. Ouchi).

0926-6410/$ - see front matter © 2004 Elsevier B.V. All rights reserved.
doi:10.1016/j.cogbrainres.2004.10.004

problem-solving processes in the brain, except for the cerebellum, in nonprofessional players [21]. Playing go is different in nature from the chess game. Chessmen have different roles in chess, but go stones all have the same value. Thus, brain activity highly depends on the contemplation of the position of the stones, not on the selection of chessman. This may result because the perception of the objects determines the actions that can be made toward them [12]. The go game, which does not involve selection of objects, may provide simpler but likely more profound cognitive processing in terms of mental imagination [7]. Obtaining a professional title depends exclusively on the period of experience, knowledge, and ability and the ability to perform mental operations that amateurs cannot attain [7]. Visuospatial processing may be greater in go experts than in novices [14]. Thus, the professional rank may be used as an index of player's ability and utilized as a covariate for examining the neural correlates of the professional go player's judgment process. One activation study of the go game was recently reported that used fMRI [6], but the study design was different from ours in subjects (amateur vs. professional and amateur) and tasks (determining next move vs. judging in different situations the correct or incorrect responses).

The purpose of the current study was to investigate neural substrates of professional strategic thinking by comparing brain activations of certificated professional go players recruited from the Japan Go Association with the neural substrates of amateurs during deliberate life-or-death (checkmate judgment) and territorial planning situations of the game using positron emission tomography (PET) with $H_2^{15}O$.

2. Materials and methods

2.1. Subjects

Eight male right-handed professional go players (mean age±S.D. 41.1±11.3 years) from Japan Go Association and six amateur go players (four male and two female, 59.5±5.4 years) gave their informed consent to participate in the present experiment, which was approved by a local ethics committee at Hamamatsu Medical Center. Professionals had experienced for more than 15 years and practiced go almost everyday for various competitions; in contrast, amateurs had experienced for more than 10 years but practiced go on a recreational basis. Each participant underwent magnetic resonance imaging (MRI) using a 0.3 T static magnet system (MRP7000AD, Hitachi, Tokyo, Japan) before PET measurement, showing no morphological abnormality. All professional players were classified by the certificated professional rank ("dan" or grade ranging from first to ninth grade), consisting of one professional player with 1-dan, one with 3-dan, one with 4-dan, one with 7-dan, one with 8-dan, and three with 9-dan.

2.2. Tasks

In the real situation of a go game, two players, sitting face to face and holding black or white stones, take turns placing stones onto one of many vacant line intersections on the board. The goal is to occupy as large an area as possible with given stones. In the present study, three situations were given to all participants. In the first task, each subject performed one baseline task; (Base) staring at the center of the go board without any thought. Then each subject performed two nonmotor cognitive tasks; (Task 1) thinking about moving stones to expand their territory in the given situation on the screen (territorial planning), (Task 2) determining the final move in a life-or-death situation in order to occupy the territory in competition (checkmate judgment) (Fig. 1A). In the two nonmotor tasks, no motor performance was allowed during the scans. In Task 1, placing stones during this stage of the go game was unlimited and there was no correct place to put the stones.

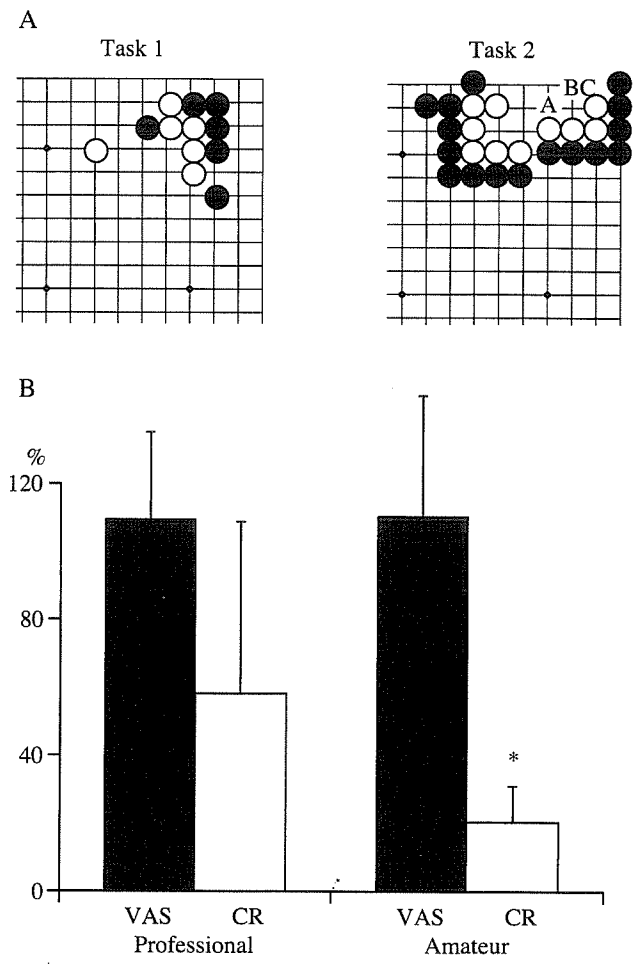

Fig. 1. Go task and task performance. (A) Examples of stones arrangement for Task 1 (territorial planning) and Task 2 (checkmate judgment), (B) visual analog scales (VAS) for task difficulty (black bar) and rates of correct answer (CR, white bar) in professional and amateur groups, which was the result of Task 2. The asterisk indicates the presence of significant difference ($p<0.05$, χ^2 test).

However, in Task 2, there was only one way to solve the problem. In Task 2, the participants were required to choose one correct answer out of three options. Three different versions of each problem and two control tasks were alternatively presented in a counterbalanced manner. Each subject was instructed to refrain from moving the eyes during tasks and the ocular movement was monitored through the video focusing on the participant's face. The amateurs performed similar tasks with easier contents designed for nonprofessionals. Each task was presented on a screen three times for 90 s. The participants were required to state their answer for each Task 2 problem and assess the difficulty for each Task 1 and Task 2 problem as a visual analog scale (VAS, from the easiest 1 to the most difficult 10) every time after completion of each scan for Task 2. The VAS value for Task 2 was defined as follows: VAS value for Task 2=(individual VAS score in Task 2)/(mean VAS score averaged between Task 1 and Task 2)×100.

2.3. Apparatus and procedure

The experiment was conducted with a brain-purpose high-resolution Hamamatsu Phtonics PET scanner [30] capable of yielding 47-slice images simultaneously with a spatial resolution of 2.9 mm (full width at half maximum) transaxially and 3.0 mm axially and with a 163-mm axial field of view. After a 10-min transmission scan for attenuation correction using a $^{68}Ge/^{68}Ga$ source with the subject's head fixed by a radiosurgery-purpose thermoplastic facemask, a 60-s emission scan was acquired from when the radiotracer first entered the cerebral circulation after intravenous bolus injection of 300 MBq of $H_2^{15}O$ [26]. The timing of the PET start to collect the rising phase of the head curve radioactivity was described previously [16]. After back projection and filtering with a Hanning filter of a cut-off frequency of 0.2 cycles per pixel, image resolution of reconstructed regional cerebral blood flow was 6.0×6.0×3.6 mm full width at half maximum and the voxel size was measured to be 1.3×1.3×3.4 mm.

2.4. Data analysis

The whole-brain CBF data were analyzed using SPM99 software (Wellcome Department of Cognitive Neurology, London, UK, http://www.fil.ion.ucl.ac/spm/spm99.html [9]). The analytic procedure of SPM was basically the same as the methods in our previous reports [16,22]. Briefly, spatially normalized data based on the standard stereotaxic brain atlas [28] after being realigned to the first image data were smoothed by an isotropic Gaussian kernel of 8 mm. The effect of variance from global CBF was excluded by proportional scaling with the global CBF normalized to 50 ml/100g/min. So, the individual rCBF response was regarded as centered adjusted rCBF value. The resultant Z-maps were displayed on the three-dimensional MRI data obtained from all participants prior to each PET session. Between-group comparison was performed using VAS as a covariate because the difficulty of go problems presented was different from each group. In correlation analyses, the ranks in professional go players were used as covariates for testing the judgment process at different stages (both Task 1 and Task 2). Significant differences in CBF between conditions were estimated with a statistical threshold set at $p<0.05$ corrected for multiple comparisons at voxel levels. In the SPM correlation analysis, statistical significance was given as $p<0.001$, uncorrected.

3. Results

3.1. Performance

There was no significant difference in VAS for task difficulty between groups. However, amateurs less frequently

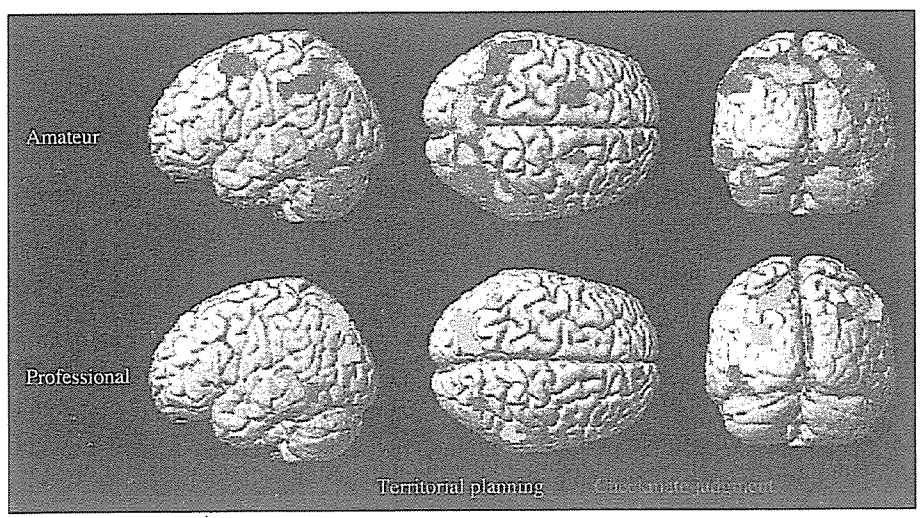

Fig. 2. Brain activation during opening stage thinking (green) (Task 1 vs. Base) and the life-or-death judgment (red) (Task 2 vs. Base) irrespective of answer content in the amateur and professional go groups ($p<0.05$, corrected). Top row: amateur, bottom row: professional. Yellow denotes an overlap of green and red areas.

Table 1
Activated brain regions in checkmate decision with and without correct answers relative to the baseline condition in professional and amateur go players

Group	Activated area	BA	Coordinates (x y z)	Z score
Successful response				
Professional	L precuneus	7	−12 −78 50	4.62
	R precuneus	7	18 −78 54	4.22
	R cerebellum (posterior lobe)	–	26 −44 −46	4.01
Amateur	Precuneus	7	0 −76 52	5.32
	R intraparietal sulcus	40/7	50 −44 42	4.98
	L precuneus	7	−16 −76 50	4.66
Failed response				
Professional	L supramarginal cortex	40	−60 −38 46	5.71
	R supramarginal cortex	40	60 −42 42	5.23
Amateur	R intraparietal sulcus	40/7	42 −52 44	6.60
	R precuneus	7	2 −76 48	6.27
	L intraparietal sulcus	40/7	−30 −60 48	5.94
	R superior precentral sulcus	6	30 −2 58	5.73
	L superior precentral sulcus	6	−24 6 58	5.39
	R middle temporal gyrus	19	42 −80 20	5.37
	L precuneus	7	−16 −72 50	5.32
	L supramarginal cortex	40	−50 −50 40	5.18

BA: Brodmann area, R: right, L: left.

made correct answers than professionals ($p<0.05$, χ^2 test) (Fig. 1B). The video showed various degrees of the eye blink and minimal eye movement during each scan in all participants, indicating that the present finding could eliminate the effect of saccadic eye movement. No motor behavior was found during scans in all subjects.

Table 2
Brain regions significantly activated during judging correctly in two groups

Group	Activated area	BA	Coordinates (x y z)	Z score
Professional	R cerebellum (anterior lobe)	–	20 −74 −18	4.73
	L cerebellum (anterior lobe)	–	−24 −76 −14	4.43
	L precuneus	7	−18 −66 60	4.36
	R cerebellum (posterior lobe)	–	36 −48 −36	4.29
Amateur	L superior precentral sulcus	6	−22 0 60	4.87
	R cuneus	17	14 −102 0	4.60
	L supramarginal cortex	40	−60 −28 40	4.53
	L superior precentral sulcus	6	26 0 64	4.51

BA: Brodmann area, R: right, L: left.

3.2. PET results

Within-subject subtraction analysis irrespective of outcome (correct or false answer) showed extensive activations in the parietal and prefrontal cortices and cerebellum bilaterally in amateur go players in either type of task (upper images, Fig. 2), whereas more focal activated regions were observed in the parietal and temporooccipital cortices and right cerebellum in the professional group (bottom images, Fig. 2). When the players made correct answers in Task 2 (checkmate judgment), the bilateral superior parietal cortices (precuneus) and the right cerebellum was activated in the professional group, and the precuneus and intraparietal sulcus region were significantly activated in amateurs (Table 1, Fig. 3, green). When thinking incorrectly, the bilateral supramarginal cortices were activated in the professional group, and the broader cortical regions covering the premotor and parietal cortices bilaterally were activated in the amateur group (Table 1, Fig. 3, red).

In the checkmate judgment process with correct response, the precuneus and cerebellar cortex were more

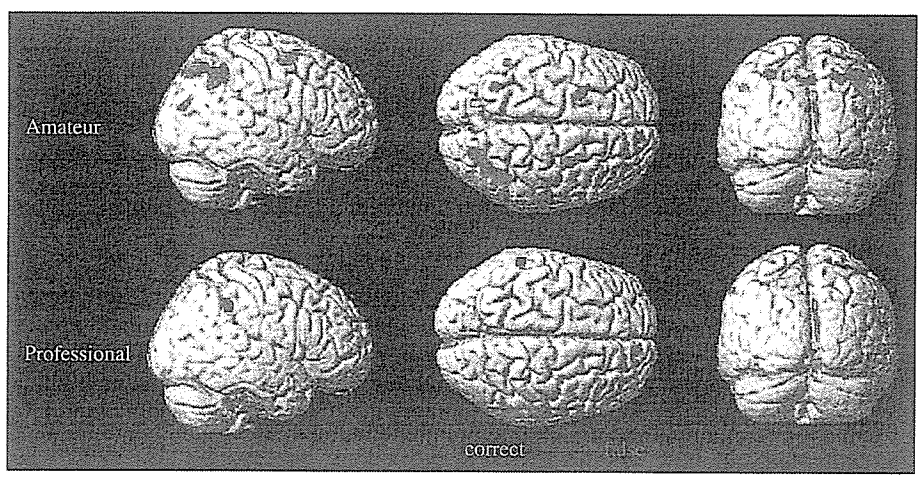

Fig. 3. Brain activation during the life-or-death deliberation with (green) and without (red) correct answers in the amateur and professional go groups ($p<0.05$, corrected). Top row: amateur, bottom row: professional. Yellow denotes an overlap of green and red areas.

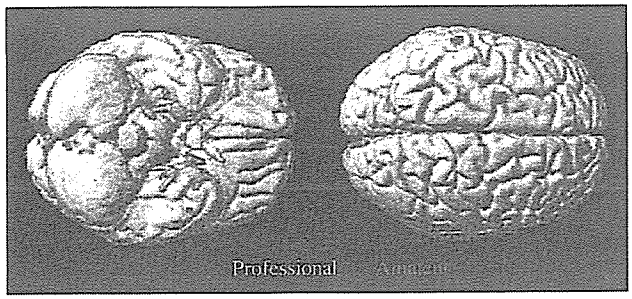

Fig. 4. Brain regions more activated during the life-or-death deliberation with correct reply in the professional than amateur group (green), and more activated in the amateur than professional group (red) ($p<0.05$, corrected).

strongly activated in the professional group, while the premotor and parietooccipital activation were stronger in the amateur group (Table 2, Fig. 4). Scattered plotting revealed that the CBF increase in the left premotor cortex correlated significantly with the task difficulty (VAS) in the amateur group (Fig. 5A, $p<0.05$, $r=0.62$), whereas the right cerebellar CBF increase correlated with the score in the professional group (Fig. 5B, $p<0.05$, $r=0.61$).

Correlation analysis in the professional group showed that the bilateral cerebellum in territorial planning (Task 1) and the right cerebellum in checkmate-decision (Task 2) correlated positively with professional ranks (Fig. 6, $p<0.001$, uncorrected).

4. Discussion

The present study revealed different neural substrates involved in cognitive processes between professional and amateur go players (irrespective of successful or failed outcome during the go game). The precuneus and cerebellum were engaged more in the checkmate judgment process in professional players, while the premotor and occipitoparietal cortices were remarkably activated in amateurs. Although unsuccessful performance caused broader brain activation during the checkmate judgment in the amateur group (Fig. 3), only focal regions were detected in the professional group, suggesting more economical use of the brain energy in professional go players. As suggested in a recent study of professional musicians [17], the different cortical representations in judgment process could be interpreted as a result of cortical plasticity in highly skilled go players.

In view of correct or incorrect responses during the game, it was found that the precuneus was significantly activated during the checkmate judgment with correct answers in both professional and amateur players. This region connects to the anterior cingulate, prefrontal, lateral parietal and temporal cortices [29]. This anatomical connection suggests that the precuneus plays a role in orchestrating multimodal associative functions. Hence, almost all the participants, when performing successfully, would have utilized every part region of the brain related to the precuneus activity. It has been reported that the precuneus is activated more during silent tasks for motor imagery [4,24] and during motor imagery of complete finger movement than during explicit execution [11]. Thus, it is suggested that the precuneus might allow complete mental reproduction of the configuration of go stones on the imagined board in the players with correct responses. The left precuneus was engaged in this strategic thinking in professional players. Therefore, one can assume that professional go players exploit this ability efficiently and make the most of the motor imagery skills through highly vigilant or conscious retrieval of acquired memory [2]. In contrast, unsuccessful deliberation caused supramarginal activation in professionals and the prefrontal-temporoparietal activation in amateurs. A recent fMRI study showed that the supramarginal cortex might be involved in an enactment effect that improves performance encoding ability [27]. This suggests that trial and error of different

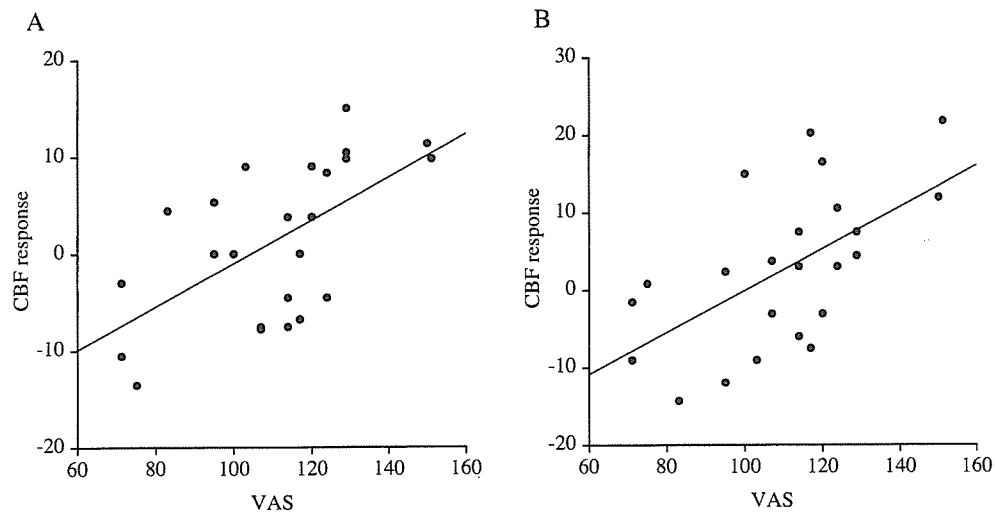

Fig. 5. Correlation analyses between VAS scores (%) and premotor CBF responses (%) in the amateur group (A) and between VAS scores and cerebellar CBF responses in the professional group (B).

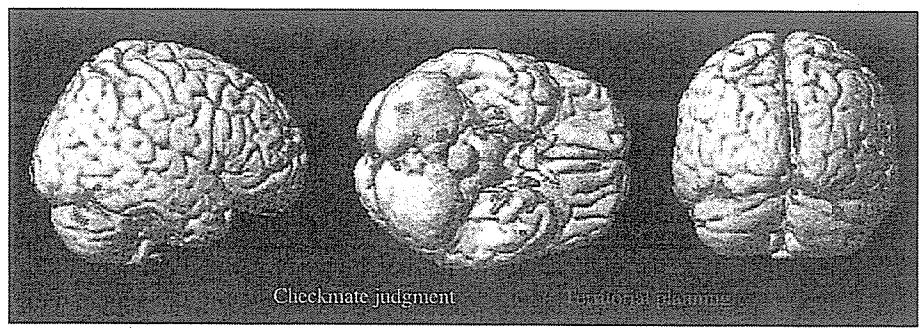

Fig. 6. Activated brain regions significantly correlated with professional "dan" ranks during the territorial planning (red) and the life-or-death judgment (green) in the professional group ($p<0.001$, uncorrected).

moves might have activated the supramarginal cortex in professional players. In contrast with the professional go players, amateur players lacking in strategic or enactment ability required incorporation of the prefrontal (premotor) and parietooccipital cortex, including the precuneus, to solve the problem (Fig. 4). This premotor activity was positively associated with the difficulty of the go problem (Fig. 5A). This pattern of activation in amateurs is consistent with the activation results in a recent fMRI study showing that the premotor and precuneus regions were activated conjointly during visuomotor operation [13] and in a chess study revealing activations of the superior frontal and occipitoparietal regions during checkmate judgment [21]. The difference of these patterns in judgment processes between professional and amateur go players may reflect a distinctive professional way of thinking leading to greater efficiency, which requires a smaller number of active neurons in specific regions incorporated in the critical situations during the go game.

Another interesting result from the comparison of the professional and amateur group in the present study was that the cerebellum was more engaged in the endgame strategy in professional players. The cerebellum has been implicated in motor imagery [8,19] and problem solving [18] in nonmotor cognitive operations. As the rank of professional go players became higher, this cerebellar cortex was more activated as shown in Fig. 6. In addition, this cerebellar activity correlated positively with VAS for task difficulty (Fig. 5B). This seemingly contradictory finding suggests that VAS of professionals in the present study might indicate uneasy emotion, because the cerebellar activation was correlated with gradual increase in task-demand during mental rehearsal [3]. Actually, some higher ranking professionals exhibited high VAS scores and excellent achievement. Thus, the cerebellum in the professional players might be associated with predictive control that guides online imagery motor performance during tense situations of the go game.

There are a few methodological caveats that have to be taken into account for the present study. The task contents in life-or-death problems given to amateurs were different from those given to professionals because amateurs would not have been able to solve the difficult tasks given to the professionals. Although the VAS for task difficulty was found similar between the groups, the strategy to solve the problem might be different. The present study did not attempt to elucidate each step of problem solving or strategic cognitive processes. This issue may be important for unraveling the mystery of the expert's mind. The questionnaire after each session of PET scans revealed that some professionals had solved the problems early within the 60-s period and spent the remaining times verifying the answer. This might cause not only weaker activation of brain region responsible for the execution of solving tasks, but also incorporation of brain regions irrelevant to the judgment process. Thus, the present result might reflect the summation of neural substrates for judgment and imagery retrieval processes occurring in the professional mind.

In summary, our results have shown that the professional judgment requires the precuneus and cerebellar activations during the go game. This suggests that visual imagery and motor imagination may be important for the highly skilled tactics of professionals. In contrast, it seems that the extensive frontoparietal regions functioning partly in visuomotor processing operate dominantly in execution of solving problems in amateur go players. In view of brain rehabilitation for the elderly and patients with dementia, playing a game of go may cause premotor activation, which may be of great value for stimulating the brain, because incorporation of the premotor region activity is necessary for executing arithmetic cognitive tasks in Alzheimer's disease patients [23]. The different pattern of cognitive processes between expert and amateur go players may reflect the brain functional plasticity or functional specialization that is acquired later in domain-specific experts.

Acknowledgments

We would like to thank Mr. Zenta Takekawa (Japan Go Association) for his task selection, Mr. Fumitoshi Nakamura and the staff of the Japan Go Association for their constant support in the present study.

References

[1] G. Allen, R.B. Buxton, E.C. Wong, et al., Attentional activation of the cerebellum independent of motor involvement, Science 275 (1997) 1940–1943.

[2] N.C. Andreasen, D.S. O'Leary, S. Paradiso, et al., The cerebellum plays a role in conscious episodic memory retrieval, Hum. Brain Mapp. 8 (1999) 226–234.

[3] H. Boecker, A.O. Ceballos-Baumann, P. Bartenstein, et al., A H(2)(15)O positron emission tomography study on mental imagery of movement sequences—the effect of modulating sequence length and direction, Neuroimage 17 (2002) 999–1009.

[4] E. Bonda, M. Petrides, S. Frey, Neural correlates of mental transformations of the body-in-space, Proc. Natl. Acad. Sci. U. S. A. 92 (1995) 11180–11184.

[5] C. Calarge, N.C. Andreasen, D.S. O'Leary, Visualizing how one brain understands another: a PET study of theory of mind, Am. J. Psychiatry 160 (2003) 1954–1964.

[6] X. Chen, D. Zhang, X. Zhang, et al., A functional MRI study of high-level cognition: II. The game of GO, Brain Res. Cogn. Brain Res. 16 (2003) 32–37.

[7] C. Cho, Go: A Complete Introduction of the Game, Kiseido Publishing, Tokyo, 1997, 1–138 pp.

[8] J. Decety, H. Sjoholm, E. Ryding, et al., Cerebellum participates in mental activity: tomographic measurements of regional cerebral blood flow, Brain Res. 535 (1990) 313–317.

[9] K.J. Friston, A.P. Holmes, K.J. Worsley, et al., Statistical parametric mapping in functional imaging: a general linear approach, Hum. Brain Mapp. 2 (1995) 189–210.

[10] J.H. Gao, L.M. Parsons, J.M. Bower, et al., Cerebellum implicated in sensory acquisition and discrimination rather than motor control, Science 272 (1996) 545–547.

[11] E. Gerardin, A. Sirigu, S. Lehericy, et al., Partially overlapping neural networks for real and imagined hand movements, Cereb. Cortex 10 (2000) 1093–1104.

[12] J. Grezes, J. Decety, Does visual perception of object afford action? Evidence from a neuroimaging study, Neuropsychologia 40 (2002) 212–222.

[13] T. Hanakawa, M. Honda, T. Okada, et al., Neural correlates underlying mental calculation in abacus experts: a functional magnetic resonance imaging study, Neuroimage 19 (2003) 296–307.

[14] T. Hatta, T. Kogure, A. Kawakami, Hemisphere specialization of Go experts in visuospatial processing, Am. J. Psychol. 112 (1999) 571–584.

[15] M. Ito, Movement and thought: identical control mechanisms by the cerebellum, Trends Neurosci. 16 (1993) 448–450.

[16] M. Iwase, Y. Ouchi, H. Okada, et al., Neural substrates of human facial expression of pleasant emotion induced by comic films: a PET Study, Neuroimage 17 (2002) 758–768.

[17] L. Jancke, N.J. Shah, M. Peters, Cortical activations in primary and secondary motor areas for complex bimanual movements in professional pianists, Brain Res. Cogn. Brain Res. 10 (2000) 177–183.

[18] S.G. Kim, K. Ugurbil, P.L. Strick, Activation of a cerebellar output nucleus during cognitive processing, Science 265 (1994) 949–951.

[19] A.R. Luft, M. Skalej, A. Stefanou, et al., Comparing motion- and imagery-related activation in the human cerebellum: a functional MRI study, Hum. Brain Mapp. 6 (1998) 105–113.

[20] E.A. Maguire, R.S. Frackowiak, C.D. Frith, Recalling routes around London: activation of the right hippocampus in taxi drivers, J. Neurosci. 17 (1997) 7103–7110.

[21] P. Nichelli, J. Grafman, P. Pietrini, et al., Brain activity in chess playing, Nature 369 (1994) 191.

[22] Y. Ouchi, H. Okada, E. Yoshikawa, et al., Brain activation during maintenance of standing postures in humans, Brain 122 (1999) 329–338.

[23] Y. Ouchi, E. Yoshikawa, M. Futatsubashi, et al., Activation in the premotor cortex during mental calculation in patients with Alzheimer's disease: relevance of reduction in posterior cingulate metabolism, Neuroimage 22 (2004) 155–163.

[24] L.M. Parsons, P.T. Fox, J.H. Downs, et al., Use of implicit motor imagery for visual shape discrimination as revealed by PET, Nature 375 (1995) 54–58.

[25] M. Pesenti, L. Zago, F. Crivello, et al., Mental calculation in a prodigy is sustained by right prefrontal and medial temporal areas, Nat. Neurosci. 4 (2001) 103–107.

[26] M.E. Raichle, W.E.W. Martin, P. Herscovitch, et al., Brain blood flow measured with intravenous H2(15)O: II. Implementation and validation, J. Nucl. Med. 24 (1983) 790–798.

[27] M.O. Russ, W. Mack, C.R. Grama, et al., Enactment effect in memory: evidence concerning the function of the supramarginal gyrus, Exp. Brain Res. 149 (2003) 497–504.

[28] J. Talairach, P. Tournoux, Co-planer Stereotaxic Atlas of the Human Brain: 3-Dimensional Proportional System: An Approach to Cerebral Imaging, Georg Thieme, Stuttgart, 1988.

[29] E.P.M. Vianna, G. Van Hoesen, J. Parvizi, Efferent connections of the primate posterior cingulate, retrosplenial and mesial parietal cortices, J. Neurosci. 587 (2002) 12.

[30] M. Watanabe, K. Shimizu, T. Omura, et al., A new high resolution PET scanner dedicated to brain research, IEEE Trans. Nucl. Sci. 49 (2002) 634–639.

ELSEVIER

NeuroImage

www.elsevier.com/locate/ynimg
NeuroImage 29 (2006) 697 – 705

Cerebral hemodynamics evaluation by near-infrared time-resolved spectroscopy: Correlation with simultaneous positron emission tomography measurements

Etsuko Ohmae,[a,*] Yasuomi Ouchi,[b] Motoki Oda,[a] Toshihiko Suzuki,[a] Shuji Nobesawa,[b] Toshihiko Kanno,[b] Etsuji Yoshikawa,[a] Masami Futatsubashi,[a] Yukio Ueda,[a] Hiroyuki Okada,[a] and Yutaka Yamashita[a]

[a]*Central Research Laboratory, Hamamatsu Photonics K.K., 5000 Hirakuchi, Hamamatsu, Shizuoka 434-8601, Japan*
[b]*Positron Medical Center, Hamamatsu Medical Center, 5000 Hirakuchi, Hamamatsu, Shizuoka 434-0041, Japan*

Received 18 August 2004; revised 3 March 2005; accepted 4 August 2005
Available online 13 September 2005

We compared pharmacologically-perturbed hemodynamic parameters (cerebral blood volume; CBV, and flow; CBF) by acetazolamide administration in six healthy human subjects studied with positron emission tomography (PET) and near-infrared (NIR) time-resolved spectroscopy (TRS) simultaneously to investigate whether NIR-TRS could measure in vivo hemodynamics in the brain tissue quantitatively. Simultaneously with the PET measurements, TRS measurements were performed at the forehead with four different optode spacing from 2 cm to 5 cm. Total hemoglobin and oxygen saturation (SO_2) measured by TRS significantly increased after administration of acetazolamide at any optode spacing in all subjects. In PET study, CBV and CBF were estimated in the following three volumes of interest (VOIs) determined on magnetic resonance images, VOI_1: scalp and skull, VOI_2: gray matter region, VOI_3: gray and white matter regions. Acetazolamide treatment elevated CBF and CBV significantly in VOI_2 and VOI_3 but VOI_1. TRS-derived CBV was more strongly correlated with PET-derived counterpart in VOI_2 and VOI_3 when the optode spacing was above 4 cm, although optical signal from cerebral tissue could be caught with any optode spacing. As to increase of the CBV, 4 cm of optode spacing correlated best with VOI_2. To support the result of TRS-PET experiment, we also estimated the contribution ratios of intracerebral tissue to observed absorption change based on diffusion theory. The contribution ratios at 4 cm were estimated as follows: 761 nm: 50%, 791 nm: 72%, 836 nm: 70%. These results demonstrated that NIR-TRS with 4 cm of optode spacing could measure cerebral hemodynamic responses optimally and quantitatively.

Introduction

Near-infrared spectroscopy (NIRS) allows simple, non-invasive measurement of the oxygenation state and hemodynamics in living tissue by utilizing the differential in absorption spectrum between oxygenated and deoxygenated hemoglobin. This field got its start from the finding by Jobsis (1977) that when a cat's head is irradiated with near-infrared (NIR) light, the intensity of the transmitted light shows changes according to the oxygen metabolic state in the tissues. Since then, there has been growing study and technique of NIRS measurement.

Making that advantage, this method has been expected for use in surgical operations (Kakihana et al., 1996; De Blasi et al., 1997) and neonate respiration care (Meek et al., 1999; Isobe et al., 2000). Besides the clinical field, topographical imaging by multi-channels measurement is being performed to observe brain activity on the cortex (Watanabe et al., 2000; Tanosaki et al., 2001).

NIRS encompasses some different techniques and analysis, and we are adopting approaches of time-resolved spectroscopy (TRS; Oda et al., 1996; Yamashita et al., 1998), phase modulated spectroscopy (PMS; Tuchiya and Urakami, 1996; Iwai et al., 2001) or spatially resolves spectroscopy (SRS; Suzuki et al., 1999) method, etc. to quantification.

In contrast to the wide applicability of NIRS to brain monitoring, fundamental and critical questions still remain to be clarified, one of which is light propagation in the human head. The effect of the various external tissues of the head such as skin, skull and cerebrospinal fluid (CSF) on photon propagation in the internal cerebral tissue has not yet been fully examined in vivo.

Several researchers (Firbank et al., 1995; Okada et al., 1997) expressed doubts about the use of NIRS on adult human heads due to problems from the multi-layered structure of the scalp, skull, CSF and the cerebral tissue. Firbank first showed that the presence of CSF had a significant effect on the light distribution. It was

* Corresponding author. Fax: +81 53 586 6180.
E-mail address: etuko-o@crl.hpk.co.jp (E. Ohmae).
Available online on ScienceDirect (www.sciencedirect.com).

1053-8119/$ - see front matter © 2005 Elsevier Inc. All rights reserved.
doi:10.1016/j.neuroimage.2005.08.008

reported that the NIRS signal from the adult human head was only 10–20% of the total signal due to the effect of CSF from the Monte Carlo simulation. These doubts are related to the essential question of where to measure using the photon, and research studies are being conducted using both simulations (Okada and Delpy, 2000, 2003a,b; Misonoo and Okada, 2001) and experimental measurements. On the contrary, several researchers (McCormick et al., 1992; Harris et al., 1994; Germon et al., 1995; Kohri et al., 2001) have reported that NIRS can detect the brain signals more specifically by increasing the optode spacing from experimental measurements.

In this study, in order to investigate the relation between the optode spacing and light sampling depth, we observed change in the cerebral blood volume (CBV) of six adult subjects by administration of a drug with simultaneous measurement of the TRS system which can measure the blood volume and the oxygen saturation (SO_2) quantitatively and positron emission tomography (PET), and we compared the CBV by TRS (TRS CBV) with CBV by PET (PET CBV) and estimated the contribution ratios of intracerebral tissue to the observed absorption change at three different wavelengths.

Materials and methods

Subjects

Six healthy male subjects (mean age, 42.6 ± 5.08; range, 37 to 51 years) were studied. Informed consent was obtained from all subjects before experiment. It was confirmed that they had no previous history of intracranial disorders and also that there were no anatomical abnormalities by making a check with a magnetic resonance imaging (MRI; 0.3 T MRP7000AD, Hitachi Ltd., Japan).

Three-wavelength TRS system

We used TRS-10 system (Hamamatsu Photonics K.K., Japan) (Oda et al., 2000) to obtain TRS-CBV in our experiment. This system uses time-correlate single photon counting (TCPC) method for measuring the temporal function of the sample. The system measures the intensity of light in a time domain and enables analysis of to the data with the time domain photo diffusion equation (Patterson et al., 1989). The block diagram of this system is shown in Fig. 1.

As the light source, this system uses semiconductor lasers called "Picosecond Light Pulser (PLP, Hamamatsu Photonics K.K., Japan)" emitting light pulses at three different wavelengths (761 nm, 791 nm, 836 nm) with a peak power of 60 mW, average power of 30 μW, the full with at half maximum (FMHM) of 100 ps and repetition frequency of 5 MHz. The detector section of this system consists of a photomultiplier tube (PMT, H6279-MOD, Hamamatsu Photonics K.K., Japan) followed by constant fraction discriminators (CFD), time-to-amplitude converters (TAC), A/D converters and histogram memories.

The system instrumental function is about 160 ps FMWH. The three PLPs emit light pulses on a time series, and the 3-wavelength optical pulses (761, 791, 836 nm) are guided into one optical fiber via a fiber coupler (CH20G-D3-CF, Mitsubishi Gas Chemical Company Inc., Japan). An optical switch (SC SERIES, JDS FITEL Inc., Canada) in this experiment selected the light irradiation point. A neutral density filter installed between the optical switch and each irradiation fiber maintained the light entering the PMT at a correct level. Each single optical fiber (GC200/250L, FUJIKURA Ltd., Japan) used for light irradiation has a numerical aperture (N.A.) of 0.25 and a core diameter of 200 μm. The optical bundle fiber (LB21E, HOYA Corp., Japan) used to collect the light has an N.A. of 0.21 and a bundle diameter of 3 mm.

TRS data analysis

The observed temporal profiles were fitted into the photon diffusion equation (Patterson et al., 1989) using the non-linear least square fitting method. The reduced scattering (μ_s') and absorption coefficients (μ_a) for three wavelengths were calculated (Appendix A). Then oxyhemoglobin (TRS HbO_2), deoxyhemoglobin (TRS Hb), total hemoglobin (TRS tHb) and oxygen saturation (SO_2) were calculated with least square method (Appendix B). We then converted the TRS tHb into the TRS CBV for comparison with the PET CBV (Appendix C). Additionally, we calculated the partial mean pathlength of extracerebral tissue (L_{ext}) at each wavelength

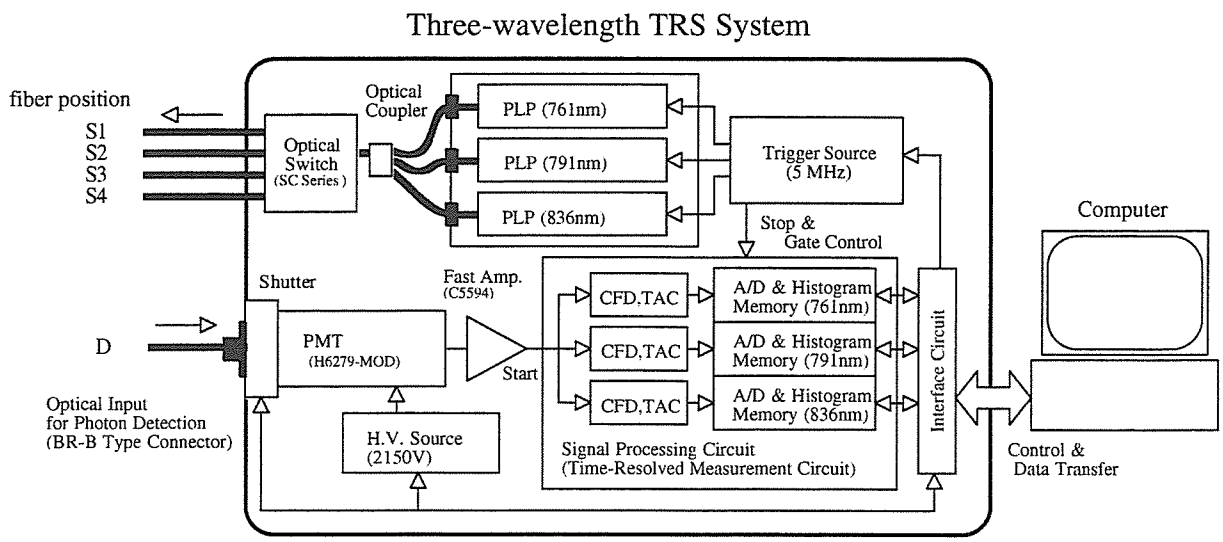

Fig. 1. Block diagram of time-resolved spectroscopy system (TRS-10: Hamamatsu Photonics K.K.).

by applying the method by the reference (Kohri et al., 2001) for five subjects whose absorption coefficients (μ_a) increased proportional to optode spacing from 2 to 4 cm. The observed mean pathlength (L_{obs}) was calculated (Zhang et al., 1998) from temporal profiles. Then, we determined the contribution ratio of the intracerebral tissue to the observed absorption change using these values.

TRS fiber position

Prior to the experiment, headgear was made for each volunteer to fix the TRS optical fibers to their left forehead. The headgear was made of thermoplastic material (ESS-15, Engineering System Co., Japan) to ensure a secure fit onto the head of each volunteer. A total of five fiber holders were fabricated for four light irradiation points (S_{1-4}) with optode spacings of 2, 3, 4 and 5 cm and one light detection point (D), and a black sheet was affixed to the inner side of the headgear except for the fiber holders to shield a detection fiber from stray light propagating on the skin surface. More specifically, the light irradiation point S_4 was first established on the left forehead, at a point 35 mm above supra-orbital margin so as to avoid the frontal sinus, and also 1 cm away from the median line to avoid the superior sagittal sinus. Next, the other light irradiation and detection points (S_{1-3}, D) were established using this point (S_4) as a reference. The positions of the light irradiation and detection points (S_{1-4}, D) on the MRI image of the head are shown in Fig. 2A. After measurement was complete, the value of optode spacing for substitution into the photon diffusion equation was measured as a straight distance with calipers. Fabricating headgear allowed the measurement to be easily made and permitted setting accurate optode spacing.

PET procedure

PET was performed using a high resolution PET scanner (SHR22000, Hamamatsu Photonics KK, Hamamatsu, Japan) (Iwase et al., 2002) with spatial resolution of 3.6 mm at full width half maximum (FWHM) transaxially and 4.2 mm axially, and with a 23-cm axial field of view, yielding 63 image slices simultaneously. After backprojection and filtering, the image resolution was 8.0 × 8.0 × 5.3 mm FWHM. The voxel of each reconstructed image measured 1.73 × 1.73 × 3.6 mm. Just prior to PET measurement, each subject underwent an MRI for determining the brain scanning area by using a static magnet with 3-dimensional mode acquisition (Ouchi et al., 1998). Fifteen-minute transmission scan for attenuation correction was performed with a $^{68}Ge/^{68}Ga$ source.

We applied the ^{15}O-CO short inhalation method followed by 5 min of data acquisition to measure the PET CBV (Lammertsma and Jones, 1983; Lammertsma et al., 1987). During this acquisition period, two pairs of arterial blood samples were collected for determining arterial ^{15}O-CO radioactivity.

One hundred twenty-second dynamic emission scans (10 s × 12 frames) were performed while subjects received a 500-MBq bolus of $H_2^{15}O$ through the right cubital vein by an automated injector. Simultaneously after injection, arterial blood was continuously withdrawn through the left brachial artery using the automated arterial blood γ-ray coincidence counter (BACC-2: Hamamatsu Photonics K.K., Hamamatsu, Japan) yielding arterial input data per second (Ouchi et al., 2001). A quantitative PET CBF value was estimated using 2-min $H_2^{15}O$ data accumulated after the tracer started circulating in the brain by summing the dynamic frames based on the autoradiographic method (Herscovitch et al., 1983).

Physiological parameters were monitored during PET examination and additional arterial blood samples were taken after each scan for analyzing levels of $PaCO_2$, Hb, hematocrit and arterial pH using a blood gas analyzer (Bayer Rapidlab 860, Tokyo, Japan). The psychophysical condition of each subject was evaluated by asking if any different sensation or mental activity was developed during the whole measurement in order to exclude any change in such brain activities as a confounding factor.

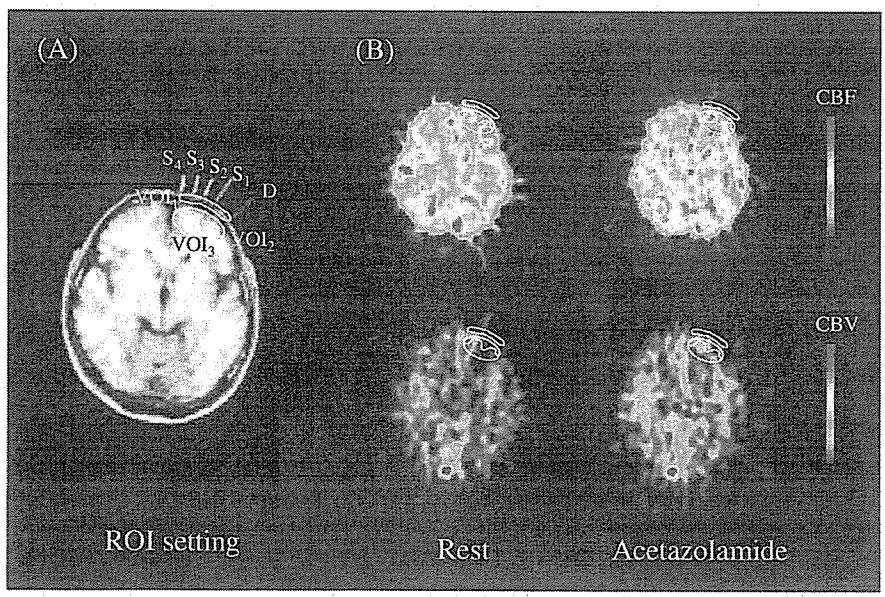

Fig. 2. Fiber and VOI positions setting on MRI image and PET images. (A) Fiber markers appear on left forehead. S_{1-4} and D are corresponding to irradiation fibers and a detection fiber, respectively. Optode spacings of S_1-D: 2 cm, S_2-D: 3 cm, S_3-D: 4 cm, S_4-D: 5 cm were set. The four PET VOIs were set as follows. VOI_1: extracerebral tissue, VOI_2: gray matter region, VOI_3: gray matter and white matter regions. (B) Images of typical measurements (41 years old; male) of PET CBF (upper) and PET CBV (lower) in the resting (left) and loading (right) state.

After measurements, to grasp the TRS light irradiation and detection points on the PET image, the fiber positions were marked by multi-modality radiographic markers (MM-3004, I.Z.I Medical Products Corp., USA) and the brain once again measured by MRI.

PET VOI

The volume of interest (VOI) on PET image used for comparison with TRS values was set by means of the following procedure. First of all, 3-dimensional MRI images were cut into 3.6 mm thick slices transversely along the multi-modality radiographic marker line. Then two slices involving these markers were selected from all these slices. Next, the following four VOIs were placed under S_4-D area on the two slices. These were set as VOI_1: extracerebral tissues (such as scalp and skull), VOI_2: gray matter region, VOI_3: gray matter and white matter regions. These VOIs were then repositioned on the PET image matching the selected two MRI slices as the PET VOIs. Mean values for each VOI size were VOI_1: 2.88 cm^3, VOI_2: 3.16 cm^3, VOI_3: 5.99 cm^3. The VOI settings are shown in Fig. 2A.

Since the PET CBF and PET CBV values were calculated with coefficients established for intracerebral tissues, the data of VOI_1 set in extracerebral tissues were treated with arbitrary unit.

Protocol

PET measurements were performed in the resting state (before administration) and the loading state (after administration) at more than 20 min after the intravenous administration of 1000 mg acetazolamide (Diamox, Japan Wyeth Ledele Ltd., Japan) appeared to be the maximum effect of cerebral vasodilatation. Two CBF measurements and one CBV measurement with PET were performed in resting and loading state.

In the TRS measurement, the optode spacings were changed in sequence by switching the four light irradiation points (S_{1-4}) with an optical switch. To maintain a peak count greater than 5000 (Suzuki et al., 1994), the acquisition times at each light irradiation point were set to 10, 20, 30 and 120 s. These TRS measurements were performed consecutively on a time series from the start to the finish of the PET measurements. Subjects were kept at rest while lying face up on the bed during measurements. The protocol is shown in Fig. 3.

Statistical analysis

All results were expressed as mean ± SD. Statistical significance of the changes in PET CBV, PET CBF, TRS CBV and SO_2 before and after administration of acetazolamide was analyzed by paired t test. Statistical significance of contribution ratio among wavelengths was analyzed by ANOVA and Bonferroni t test. A significant difference was defined when statistical probability: P was less than 0.05.

The association between TRS CBV and PET CBV was evaluated by squared Pearson's correlation coefficient (r^2). Change in CBV (ΔCBV) by administration of acetazolamide was also evaluated in the same way. The assessment for VOI_1 was not performed because it was expressed in the arbitrary unit. Statistical significance of r^2 was analyzed by a t test for r^2. A significant difference was defined when statistical probability: P was less than 0.05.

Results

Physiology

There were no significant changes in physiologic parameters (arterial blood pressure, pulse rates, $PaCO_2$) and psychophysical states (changes in mental activity) between before and after administration of acetazolamide (data is not shown).

TRS

Typical values of TRS tHb and SO_2 at each optode spacing during the experiment are shown in Fig. 4. The rise of TRS tHb and SO_2 was confirmed at all optode spacings immediately after administering acetazolamide and reached a plateau after about 10 min. These phenomena were observed in all subjects.

Mean values of TRS CBV and SO_2 at each optode spacing in the resting and loading states are shown in Fig. 5. The TRS CBV and SO_2 at each optode spacing in resting state were as follows: 2 cm: 2.7 ± 0.4 cm^3/100 g, 70.3 ± 1.1%, 3 cm: 3.0 ± 0.2 cm^3/100 g, 68.7 ± 1.8%, 4 cm: 3.0 ± 0.3 cm^3/100 g, 69.6 ± 2.3%, 5 cm: 2.7 ± 0.3 cm^3/100 g, 71.7 ± 2.8%. The TRS CBV and SO_2 in loading

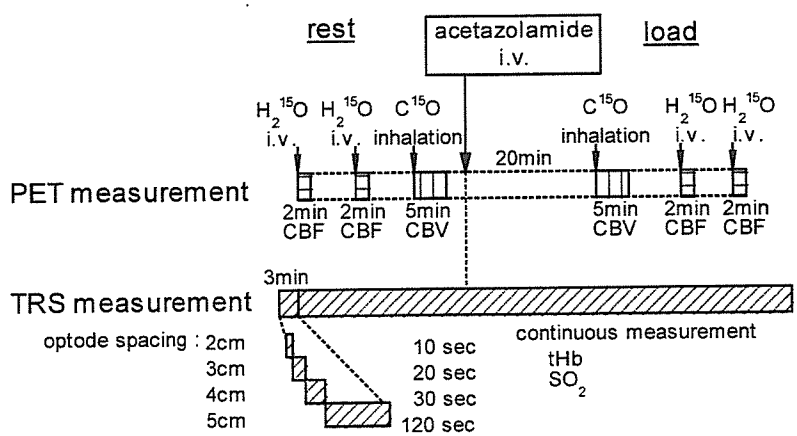

Fig. 3. TRS and PET simultaneous measurement protocol. The TRS measurement was made while switching the light irradiation point to set optode spacings of 2, 3, 4 and 5 cm. Data acquisition time was 10, 20, 30 and 120 s at each irradiation point. In the PET measurement, CBF was measured twice and CBV once, both resting and loading state. One CBF measurement required 2 min and the CBV measurement 5 min.

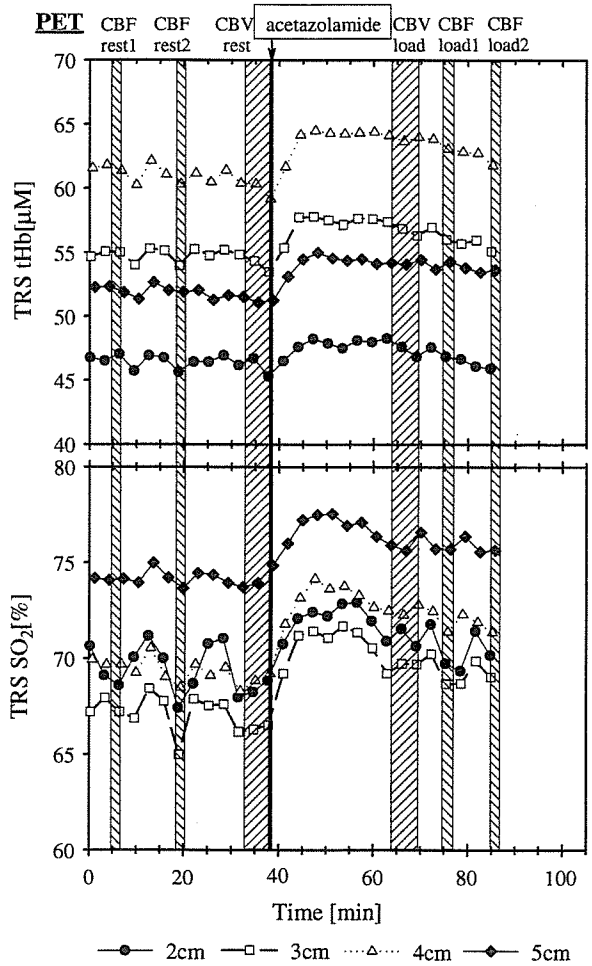

Fig. 4. TRS measurement results at each optode spacing. Typical responses (41 years old; male) of TRS tHb (upper) and SO_2 (lower) for acetazolamide administration. The oblique lines indicate PET data acquisition period.

state significantly rose approximately 6% and 3%, respectively, of resting state at all optode spacing.

PET

The CBF and CBV images at the resting and loading state are shown in Fig. 2B. The CBF can be clearly seen to increase after administering acetazolamide, whereas the CBV shows a relatively minor increase.

Mean values of PET CBF and PET CBV at each VOI in the rest and loading state are shown in Fig. 6. The PET CBF and PET CBV at each VOI in the resting state were as follows: VOI_1 (arbitrary unit): 6.6 ± 1.2 cm^3/100 g/min, 2.6 ± 0.4 cm^3/100 g, VOI_2: 39.6 ± 5.3 cm^3/100 g/min, 4.4 ± 0.9 cm^3/100 g, VOI_3: 40.6 ± 5.1 cm^3/100 g/min, 4.0 ± 0.7 cm^3/100 g. The PET CBF and PET CBV at $VOI_{2,3}$ in the loading state significantly increased approximately 30% and 10%, respectively, compared to those of resting state. However, no significant increases were observed for the CBF and CBV at VOI_1, which increased 8.2% and −1.3%, respectively.

Correlations

The r^2 for the CBV and ΔCBV, respectively, between TRS and PET are shown in Tables 1A and B.

The r^2 of CBV at 4 cm and 5 cm of optode spacing was higher than those at 2 cm and 3 cm of optode spacing at all VOI, and they also showed high correlation values as the depth increased.

As to ΔCBV, r^2 of VOI_2 showed exceptionally higher than those of VOI_3 at all optode spacing. At the VOI_2, however, r^2 at 2 cm of optode spacing showed lower than those at other optode spacing. At the VOI_3, just as with the CBV correlation, r^2 at 4 cm and 5 cm of optode spacing showed higher than those at 2 cm and 3 cm of optode spacing.

L_{ext} and the contribution ratio

L_{ext} at each wavelength was as follows: 761 nm 11.7 ± 2.7 cm, 791 nm: 6.3 ± 2.4 cm, 836 nm: 6.5 ± 1.5 cm. L_{ext} at 761 nm was significantly longer than those of 791 and 836 nm, against

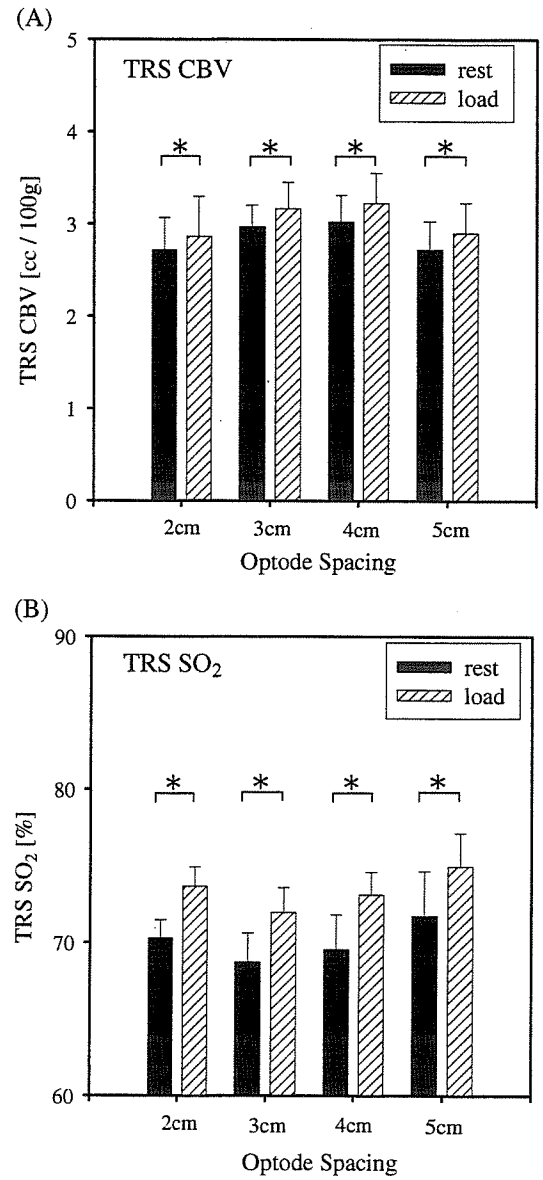

Fig. 5. Mean values (n = 6) for (A) TRS CBV and (B) SO_2 in the resting and loading state. Significant differences were confirmed for all optode spacings after administering acetazolamide (*P < 0.05).

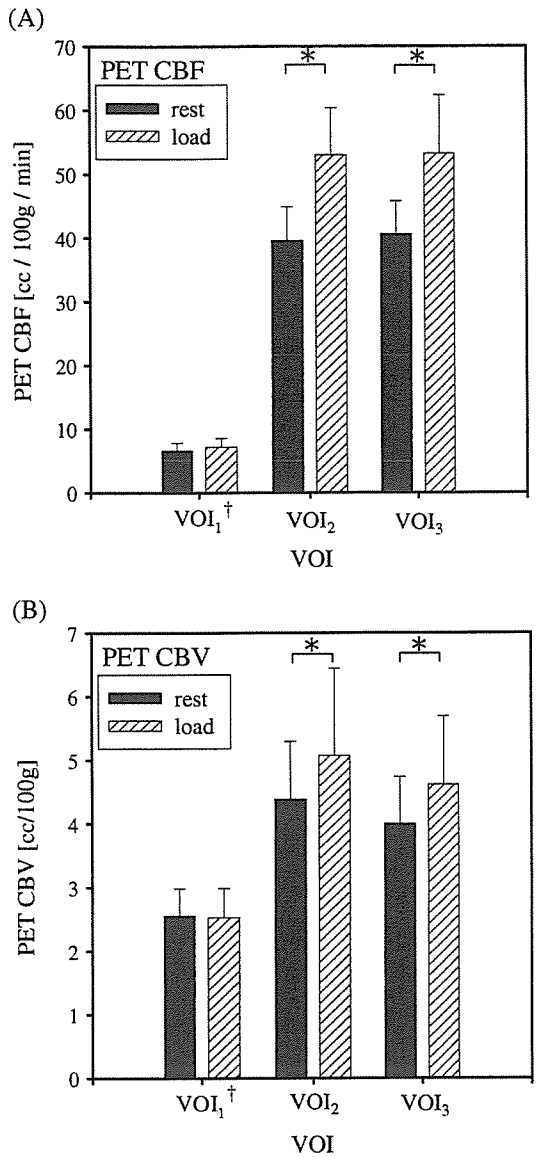

Fig. 6. Mean values (n = 6) for (A) PET CBF and (B) PET CBV in the resting and loading state. Significant differences were confirmed at VOI_2 and VOI_3 after administering acetazolamide (*P < 0.05). †VOI_1 was expressed in the arbitrary unit.

observed mean pathlength of each wavelengths were also the same (data is not shown).

The contribution ratios of the cerebral tissue at each wavelength are shown in Fig. 7. The contribution ratios of 761 nm with all optode spacing were significantly lower than those of 791 and 836 nm.

Discussion

The acetazolamide used in this experiment increases the regional CBF by inhibiting carbonic anhydrase and thereby expanding cerebral blood vessels (Posner and Plum, 1960; Ehrenreich et al., 1961). This drug is therefore generally used to assess the cerebrovascular reserve capacity as an acetazolamide test. Similarly in this study, significant increases of PET CBF and PET CBV by

Table 1
Squared correlation coefficient (r^2) between PET and TRS: (A) CBV; (B) ΔCBV

TRS optode spacing	PET	
	VOI_2	VOI_3
(A) r^2: TRS CBV vs. PET CBV (n = 6)		
2 cm	0.601**	0.535**
3 cm	0.410*	0.525**
4 cm	0.690**	0.841**
5 cm	0.762**	0.859**
(B) r^2: TRS ΔCBV vs. PET ΔCBV (n = 6)		
2 cm	0.331	0.050
3 cm	0.633*	0.277
4 cm	0.699*	0.457
5 cm	0.585	0.352

* $P < 0.05$.
** $P < 0.01$.

acetazolamide in the intracerebral tissues ($VOI_{2,3}$) and no significant increase of those in the extracerebral tissues (VOI_1) were confirmed. In the TRS measurements on the other hand, significant increases in CBV at all optode spacings were observed. Further, the result of significant increases of SO_2 at all optode spacing agrees well with a report (Vorstrup et al., 1984) that there was hardly any change in $CMRO_2$ even though the CBF increased when acetazolamide was administered. These results suggest that when optode spacing is 2 cm to 5 cm, the photons passing through the head convey the intracerebral hemodynamic response.

However, the CBV and ΔCBV correlations clearly differed according to the optode spacing and VOI. As for CBV correlation, these trends suggest that the longer the optode spacing, the deeper the region that the photons can penetrate, because the correlation with VOI_3 was higher than that with VOI_2 at each optode spacing except at 2 cm. In addition, correlations at 4 cm and 5 cm of optode spacing showed a trend to higher than those at 2 cm and 3 cm of optode spacing with both VOIs. These results suggested that optode spacing was preferably more than 4 cm for improving quantification of NIR-TRS to cerebral hemodynamics.

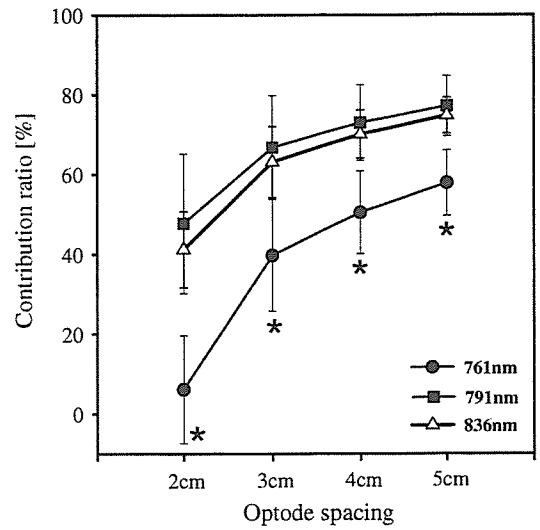

Fig. 7. Mean values (n = 5) for contribution rations of the cerebral tissue to observed absorption change. Significant differences were confirmed for all optode spacing at 761 nm to 791 and 836 nm (*P < 0.05).

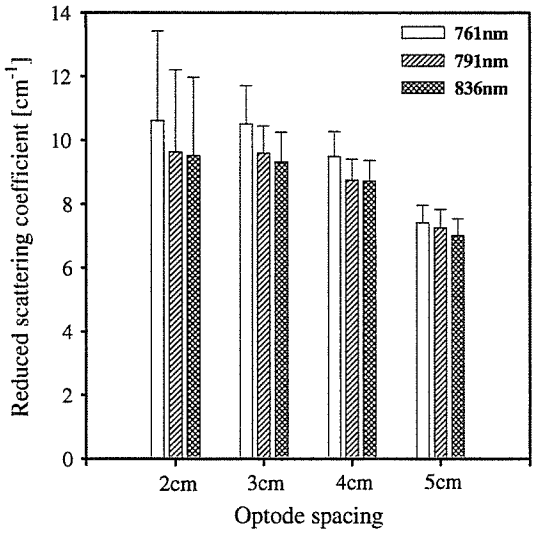

Fig. 8. Mean values (n = 5) for reduced scattering coefficient at each wavelength and optode spacing. The values of 761 nm for all optode spacing were highest among three wavelengths (no significant differences).

Because the density of blood vessels in VOI_2, which covers the gray matter mostly, was high, there might be a large increase in blood volume. Accordingly, the ΔCBV correlation with VOI_2 may be higher than VOI_3 regardless of the optode spacing. Also, the ΔCBV correlation for VOI_2 is a maximum at 4 cm of optode spacing so that this distance may be optimum for capturing cerebral hemodynamics response around the gray matter region.

Contribution ratios at 4 cm of optode spacing were as follows: 761 nm: 50.4 ± 10.3%, 791 nm: 72.9 ± 9.4%, 836 nm: 70.0 ± 6.0%. The results at 836 nm are very much in agreement with the results at 834 nm by Kohri (Kohri et al., 2001). But these results are different from previous simulation work (Firbank et al., 1995). The photon propagation depends heavily on the optical parameters of tissues. We believe that the μ_a and μ_s' of the postmortem adult human brain (Van der Zee et al., 1992) and piglet (Firbank et al., 1993) used in the simulation work maybe different from those in living tissues. Furthermore, both contribution ratios at 5 cm of optode spacing were higher than those at 4 cm and the ΔCBV correlation at 5 cm of optode spacing is lower than that at 4 cm; thus it is speculated that photons has penetrated even deeper, and contains information not only on gray matter but also on white matter and cerebral ventricle. Conversely, the lowest value of the ΔCBV correlation at 2 cm of optode spacing corresponds with derived low contribution ratios. So the 2 cm of optode spacing is not recommended for acquiring intracerebral information. Although we treated a complex layered structure as a single set of μ_a and μ_s', assuming of a homogeneous medium, making optode spacing longer could satisfy this condition concededly.

L_{ext} at 761 nm was 1.7 times of those at 791 and 836 nm, although observed mean pathlength at each wavelength was also the same values. It means that the photons of 761 nm are hard to penetrate into the cerebral tissue than those of 791 and 836 nm. To support this result, mean values for μ_s' at each wavelength and the optode spacing in the resting state are shown in Fig. 8. As the higher the scattering, the photons are harder to spread into the cerebral tissue deeply. The difference of μ_s' among wavelength showed a similar tendency to that of L_{ext}. It was also reported that the value of μ_s' increases progressively with decreasing wavelength (Bevilacqua et al., 1999; Torricelli et al., 2001). To improve the accuracy of NIR measurement, it should be necessary to consider wavelength selection including μ_s' as well as absorption spectra of hemoglobin.

The TRS system has a potential to quantitate the hemoglobin concentration since it directly measures the optical pathlength distribution of detected photons passing through the living tissue, different from the conventional measurement methods (Brazy et al., 1985; Ferrari et al., 1987; Cope and Delpy, 1988). This allows making patient-to-patient comparisons and comparing the patient condition before and after treatment, making it highly valuable as an indicator for diagnosis and treatment. In this study, a good correlation coefficient was obtained between TRS-derived CBV and PET-derived CBV, while the absolute CBV levels by TRS were lower than those by PET. One reason for the under-/over-estimation of the CBV values might be a difference in modalities which measure different in vivo responses. An absolute value of CBV weighs considerably in the NIRS study. Thus, further studies are needed to resolve this methodological issue.

NIR measurement is proven capable of continuous measurement with high time resolution while also being a simple, safe and non-invasive method. Additionally, study of diffuse optical tomography is being proceeded based on this technology (Ueda et al., 2001; Hillman et al., 2001). We hope to further develop our work in the NIRS field to the level where it can be used as a modality to assist and complement PET technology.

Conclusion

We observed a change in the CBV by administration of acetazolamide with simultaneous measurement of TRS and PET. These experiments showed that intracerebral hemodynamics response by administering acetazolamide could be captured at optode spacings of 2 cm to 5 cm.

Furthermore, by evaluating the correlation with PET, we concluded that more than 4 cm of optode spacing is preferable for improving quantification of the NIR-TRS measurement to intracerebral hemodynamics. Additionally, 4 cm of optode spacing is a good setting to monitor cerebral hemodynamics response around the gray matter region. Contribution ratio of intracerebral tissue at 4 cm estimated about 70%, although it varies according to wavelength. NIR measurement is a simple and easy method to evaluate cerebral hemodynamics.

Acknowledgments

The authors would like to thank Mr. T. Hiruma for his constant support and encouragement. The authors are also grateful to Drs. Y. Tsuchiya and T. Yamashita for useful discussions.

Appendix A. Derive reduced scattering and absorption coefficients from temporal profiles

Behavior of photon within scattering and absorption media like a living body is expressed by the photon diffusion Eq. (1) (Patterson et al., 1989).

$$\frac{1}{v}\frac{\partial}{\partial t}\phi(r,t) - D\nabla^2\phi(r,t) + \mu_a\varphi(r,t) = S(r,t) \quad (1)$$